

## Effect of Grain Size on the Thermomechanical Properties of $\text{Al}_2\text{TiO}_5$ Ceramics

Ik Jin Kim, Oh Seong Kweon, Young Shin Ko\* and Constatin Zografou

*Institute for Processing and Application of Ceramics, IPAC,*

*Dept. of Mat. Science and Engineering, Hanseo University, Seosan 352-820, Korea*

*\*Department of Science Education, Seoul National University of Education, Seoul 137-070, Korea*

(Received December 2, 1996)

The thermomechanical properties of materials from the system  $\text{Al}_2\text{O}_3$ - $\text{SiO}_2$ - $\text{TiO}_2$  (Tialite-Mullite) were investigated by correlating the thermal expansion anisotropy, flexural strength and Young's modulus with grain size and structural microcracking during cooling. Microcracking temperatures were determined by measuring the hysteresis of the thermal expansion anisotropy with dilatometry. Single phase Aluminium Titanate is a low strength material, while composites with more than 10 vol% mullite as second phase enhance the Young's modulus, thermal expansion coefficient and room temperature strength.

**Key words :** Thermal expansion, Microcracking, Hysteresis, Anisotropy,  $\text{Al}_2\text{TiO}_5$

### I. Introduction

In  $\text{Al}_2\text{TiO}_5$  polycrystalline ceramics, the thermal expansion anisotropy of three crystallographic directions causes grain boundary microcracking.<sup>1)</sup> These microcracks often result in negative thermal expansion coefficients accompanied by pronounced hysteresis.<sup>2,3)</sup> Such anisotropy creates complicate internal stresses during cooling from the sintering temperature.<sup>4)</sup> The magnitude of such stresses is a direct function of the degree of anisotropic thermal expansion, which is sufficient to exceed the intrinsic fracture strength of the material. This results in severe microcracking at room temperature and consequently the low mechanical strength and low Young's modulus.<sup>5,6)</sup> The development of microcracks also accounts for the low thermal expansion coefficients which are in reality a bulk average value based on the behaviour of individual grains. Thus the true thermal expansion coefficient of aluminium titanate is near to  $9.7 \times 10^{-6} \text{K}^{-1}$ :  $\alpha_a = 9.8 \times 10^{-6} \text{K}^{-1}$ ,  $\alpha_b = 20.6 \times 10^{-6} \text{K}^{-1}$ ,  $\alpha_c = -1.4 \times 10^{-6} \text{K}^{-1}$ .<sup>7,8)</sup>

Low thermal expansion coefficient, low Young's modulus, good thermal insulation, and excellent thermal shock resistance are characteristics of aluminum titanate ceramics. These properties, if property adjusted, allow for the insert-casting of ceramic portliners into the cylinder head [alloy AlSi 12(Cu) or cast iron], where they serve as a thermal insulation of the exhaust gas as a means of improving thermal efficiency. It is also under serious consideration for use as exhaust manifold inserts, piston crowns and turbocharger liners.<sup>9,10)</sup> Additionally it finds application in the non-ferrous metallurgical industries.<sup>11)</sup> Successful application of the material has depended on the ability to control the microcracking

phenomena and use it to advantage, together with an ability to understand the decomposition behaviour.

In this paper, the relation between grain size, grain boundary microcracking temperature and thermomechanical properties in Aluminium Titanate-Mullite (AT-M) ceramics has been investigated. AT-M composites with a wide range of composition (up to 70% mullite) were studied with the aim to enhance the thermomechanical properties of pure  $\text{Al}_2\text{TiO}_5$ .

### II. Experimental

Tetraethylorthosilicate  $\text{Si}(\text{OC}_2\text{H}_5)_4$  (Hüls AG), Ethyltitanate  $\text{Ti}(\text{OC}_2\text{H}_5)_4$  (Hüls AG),  $\alpha$ - $\text{Al}_2\text{O}_3$  (A-16 AG SG; mean particle diameter: 0.3-0.5  $\mu\text{m}$ : Alcoa Chem.), and Ethanol (Merck) were used as starting materials.  $\text{Al}_2\text{TiO}_5$ -Mullite powders were prepared by stepwise alkoxide hydrolysis of a molar ratio  $[\text{H}_2\text{O}]/[\text{Si}(\text{OC}_2\text{H}_5)_4]$  of 80 and  $[\text{H}_2\text{O}]/[\text{Ti}(\text{OC}_2\text{H}_5)_4]$  of 4 in  $\alpha$ - $\text{Al}_2\text{O}_3$  powder ethanolic solution.

Typical concentration of final solution were 0.4 mol  $\text{Si}(\text{OC}_2\text{H}_5)_4$ , 0.3 mol  $\text{Ti}(\text{OC}_2\text{H}_5)_4$ , 1.91 mol  $\text{NH}_3$ , and 33.2 mol  $\text{H}_2\text{O}$ . The solution of coated powder was then centrifuged to remove the alcoholic solution, then washed with deionized water and redispersed in aqueous  $\text{NH}_4\text{OH}$  solution (pH=10). Powder compacts were prepared by centrifugal casting and dried at room temperature for one day. The average grain sizes from the fracture surface were measured by the linear-intercept method<sup>12)</sup> using the scanning electron microscope.

The thermal expansion hysteresis (RT-1500°C) was determined using a nonloading-type dilatometer. Both heating and cooling rates were 10°C/min in air. The specimen size was 5×5×25 mm. The thermal shock resistance of

the specimens was determined by a water quenching process specified in the German industrial standard.<sup>13)</sup> Three specimens per composition were heated to 950°C for 15 min in a muffle furnace and quenched with flowing water at 20°C for 15 min. After drying at 110°C for 30 min., all specimens without spontaneously developed major cracks were subjected to the measurement of flexural strength ( $7 \times 7 \times 70$  mm) by using a universal-type testing machine. The span length was 40 mm and the cross head speed was 0.2 mm/min. The Young's modulus was measured by the resonance frequency method.

### III. Results and Discussion

Table 1 shows the phase composition and the physical properties of the specimens sintered at 1600°C for 2 hrs. The density of ATM-specimen increases with mullite content up to 20 vol% and then decreases. The ATM2, ATM3, ATM5, and ATM7 compositions reached a density level of between 88.0% and 99.9% of the theoretical density, consisting of mainly two crystalline phases: stabilized aluminium titanate and mullite. The grain size of  $\beta\text{-Al}_2\text{TiO}_5$  in composites and the amount of porosity in ATM-materials decreased with increasing mullite content. The observed increase in the relative density and thermal expansion coefficient are listed in Table 2.

Micrographs of fracture surface of the specimens sintered at 1600°C for 2 hrs are shown in Fig. 1.

The microstructure of single phase aluminium titanate consists of narrowly distributed  $\text{Al}_2\text{TiO}_5$  grains in the range of 0.5  $\mu\text{m}$ . The microstructure is intergranular microcracked, as expected due to the presence of the highly

anisotropic  $\beta\text{-Al}_2\text{TiO}_5$  crystals.

Extensive grain boundary cracking is prevalent in ATM1 materials with large grain sizes (50  $\mu\text{m}$ ), as shown in Fig. 1(b). The existence of an extensive network of these intergranular microcracks is verified by many corollary property changes, e.g. thermal expansion behavior, the elastic modulus, and flexural strength. ATM specimens containing 10 vol% mullite exhibit rapidly grain growth of the  $\text{Al}_2\text{TiO}_5$  grains and leads to an enlargement of hysteresis areas but reduced thermal expansion (Fig. 2). The materials (AT and ATM1) show low thermal expansion at 900-1000°C, but as the temperature is raised the hysteresis increases markedly. This is ascribed to the onset of mechanical healing of microcracks above 900°C on heating and their reopening or refracturing on cooling being delayed until the temperature reaches below 800°C. It is pronounced that stresses in the microstructure of all composites build up only below about 800°C.<sup>14)</sup>

Specimens of ATM2 and ATM3 appear to have a mean grain size of  $\beta\text{-Al}_2\text{TiO}_5$  ranging from 5  $\mu\text{m}$  to 20  $\mu\text{m}$ . Interlinked fine-mullite particles at grain boundaries would inhibit the grain growth of  $\beta\text{-Al}_2\text{TiO}_5$ . The grain size of aluminium titanate is decreased with increasing mullite content and the grains are surrounded by microcracks, as shown in Fig. 1(c), (d).

The difference in the microcracking temperature, such as 800, 700, 700 and 550°C for the specimens ATM1, ATM2, ATM3 and ATM5, respectively, was caused by the difference in grain size of  $\beta\text{-Al}_2\text{TiO}_5$  and mullite content.

The thermal expansion coefficients of ATM specimens lies between 0.5 and  $2.0 \times 10^{-6} \text{ K}^{-1}$  (RT-1200°C). This can

**Table 1.** Phase Compositions and Physical Properties of AT-ATM Specimens Sintered at 1600°C for 2 hrs

Materials	Mullite content vol%	Phase composition	Bulk density ( $\text{g/cm}^3$ )	Relative density (%)	Porosity (%)	Shrinkage (%)
AT	0	AT+R+C	2.9	76.0	24.0	15.0
ATM1	10	AT+Mullite+L	3.3	88.2	11.8	15.4
ATM2	20	AT+Mullite	3.5	93.3	6.7	21.3
ATM3	30	AT+Mullite	3.3	88.0	12.0	16.6
ATM5	50	AT+Mullite	3.4	92.2	7.0	16.7
ATM7	70	AT+Mullite	3.3	99.9	0	15.2

AT;  $\beta\text{-Al}_2\text{TiO}_5$ , R; Rutile, C; Corundum, L; Liquid phase, synthesized crystalline mullite vol%.

**Table 2.** Thermal Expansion Behavior and Median Grain Size of Aluminium Titanate-Mullite Composites, after Sintering at 1600°C for 2 hrs

Materials	Thermal expansion coefficient $\alpha_{20^\circ\text{C}-1500^\circ\text{C}}$ ( $10^{-6} \text{ K}^{-1}$ )	Hysteresis area ( $\text{mm}^2$ )	Microcracking temperature ( $^\circ\text{C}$ )	Average grain size (AT) ( $\mu\text{m}$ )
AT	1.8 (0.68)*	235	800	20
ATM1	0.5 (0.50)*	580	800	40
ATM2	1.6 (0.9)*	305	700	15
ATM3	2.4 (1.8)*	345	700	15
ATM5	2.3 (2.0)*	210	550	10
ATM7	7.0 (5.2)*		-	5

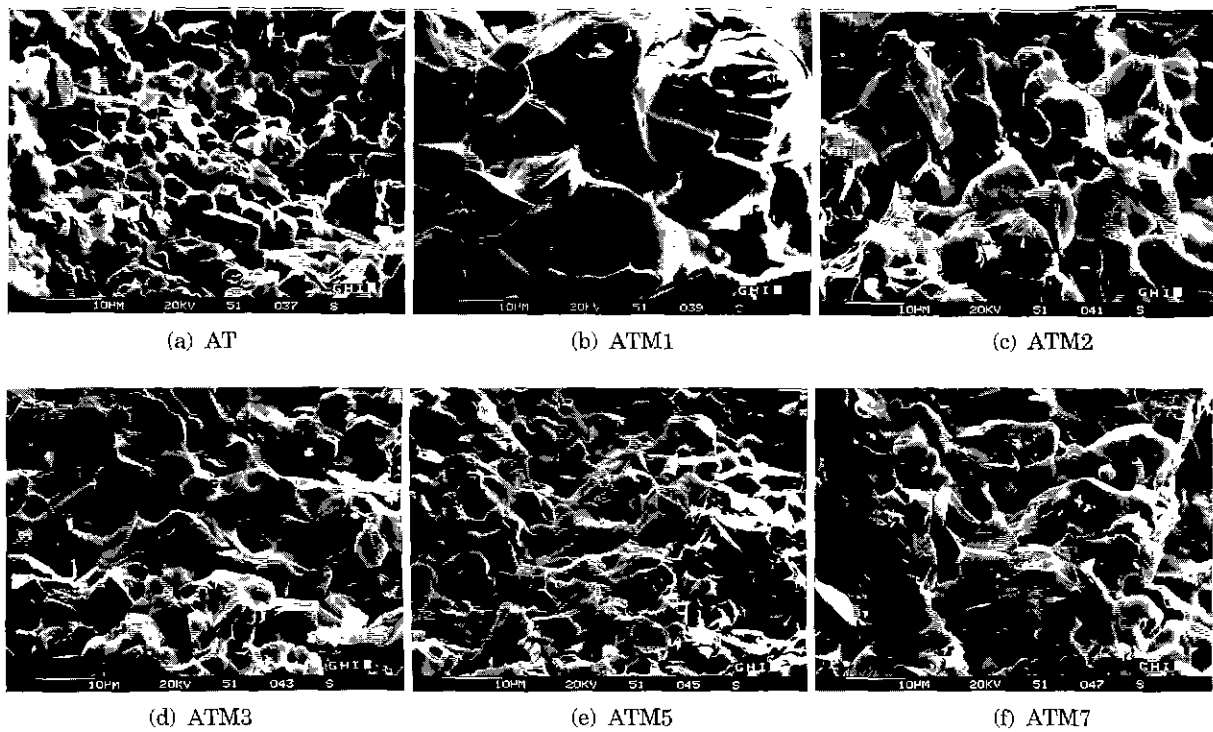


**Fig. 1.** Scanning electron micrographs of fracture surface of aluminium titanate-millite composites sintered at 1600°C for 2 hrs.

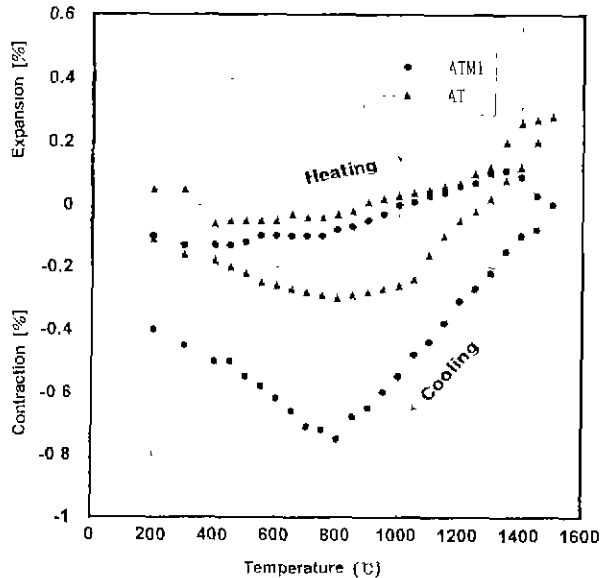


**Fig. 2.** Thermal expansion curves of AT and ATM1.

be compared with a theoretical expansion coefficient for single phase  $\beta$ - $\text{Al}_2\text{TiO}_5$  of  $9.7 \times 10^{-6} \text{ K}^{-1}$ .<sup>47</sup>

It is the pronounced thermal expansion anisotropy of the individual  $\text{Al}_2\text{TiO}_5$  grains that gives rise to internal stresses on a microscopic scale during cooling from the firing temperature.

These localized internal stresses are the driving force for microcrack formation. During reheating run, the individual crystallites expand at the lower temperatures, thus the solid volume of sample expands to the smaller

sized microcracks, while the macroscopic dimensions remain almost constant. As a result, the material expands very little. The higher the temperature, the more cracks are closed, the steeper the thermal expansion curve. However, even at 1200°C the slope is far below the theoretical value, suggesting that a lot of fraction of the microcracks is still open.

The thermal expansion curves of ATM2 and ATM3 demonstrated nearly the same hysteresis with internal rupture or microcracking created during cooling (Fig. 3). This is in good agreement with the data obtained from estimations of the  $\text{Al}_2\text{TiO}_5$  grain size of 15  $\mu\text{m}$  (see Table 1); One can clearly recognize the distinct microcracks network. The grain size of  $\beta$ - $\text{Al}_2\text{TiO}_5$  in the composites decreased with increasing mullite content. These materials have lower positive expansion temperature during heating and lower microcracking temperature during cooling of 500°C (ATM5) or not (ATM7), respectively (Fig. 4). The microcracking existing in the material are responsible for the low mechanical strength on the one hand and, on the other hand, they give the material a kind of quasi-elasticity.

Figure 5 shows the residual flexural strength of specimens having various compositions after water quenching. Relatively high strength of 72 MPa was found in specimens having 10 vol% mullite, even though this material was still only 88.2% dense. However, it gives a sudden decrease of strength after one quenching cycle, but had moderate thermal shock resistance. Average strengths of the materials having 80, 70, and 50 vol% aluminium titanate ranged from 31 to 47 MPa at room temperature

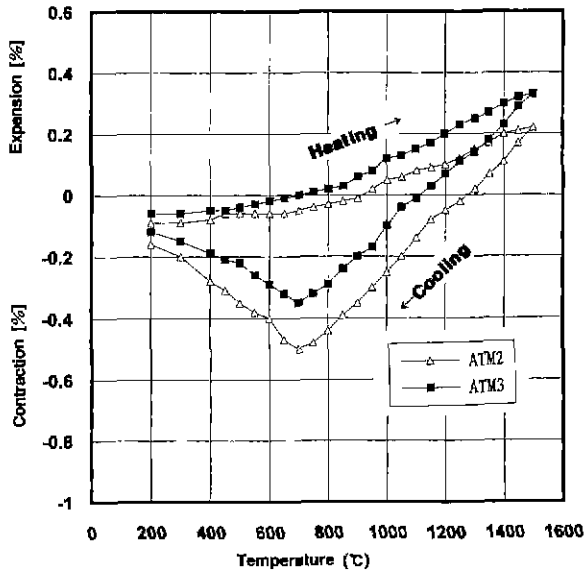


Fig. 3. Thermal expansion curves of ATM2 and ATM3.

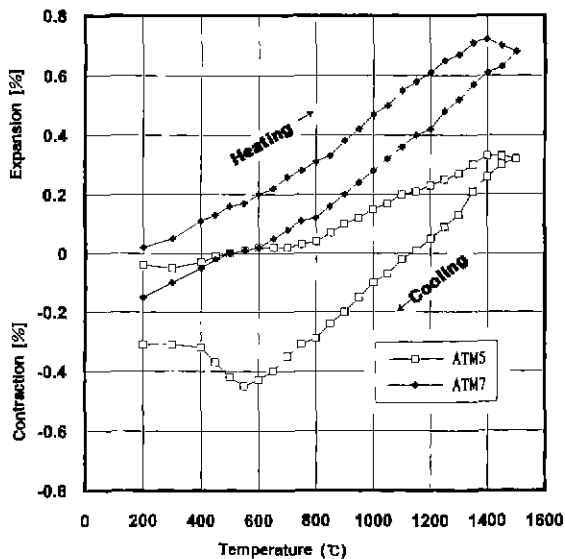


Fig. 4. Thermal expansion curves of ATM5 and ATM7.

and 30-47 MPa after 12 water quenching cycles. The strength values of ATM2 and ATM3 showed no distinct influence on quenching behaviour at 950°C and therefore they had excellent thermal shock resistance.

As shown in Fig. 6, the Young's modulus was measured as a function of quenching cycles by the resonance method. One having 10 vol% mullite has higher Young's modulus of 50 GPa than the others, which whilst denser, contained appreciable amounts of cracks in their grain boundaries. Young's moduli of the ATM2-, ATM3- and ATM5-composites containing grain boundary microcracks would be caused by the constants in the area of contact across the sintered grain boundaries. The higher microcrack density also results in better resistance to the critical thermal shock.<sup>15)</sup> The porosity dependence of the

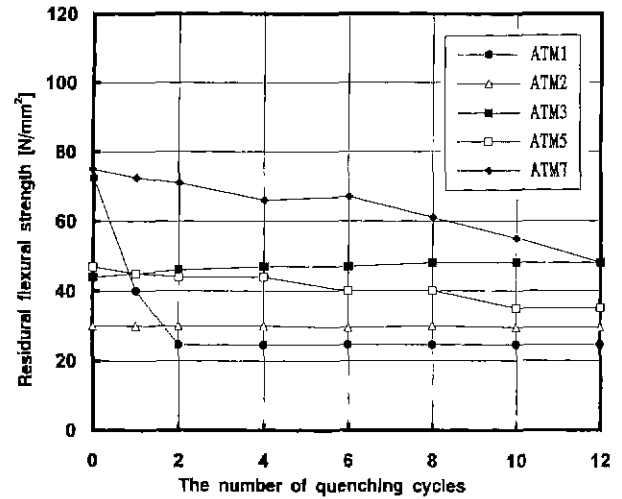


Fig. 5. Residual flexural strengths of  $Al_2TiO_5$ -mullite composites after thermal shock cycling.

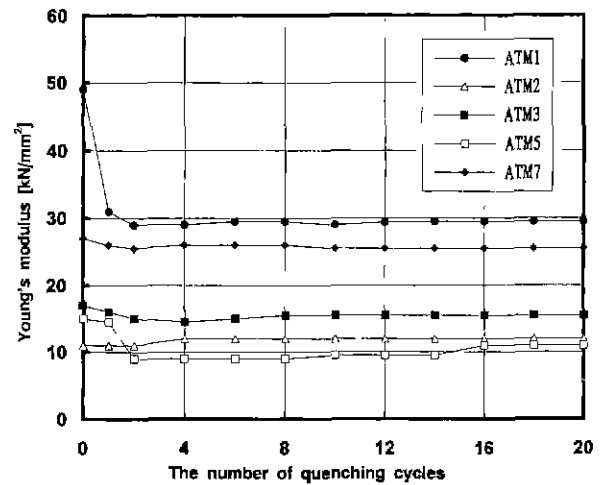


Fig. 6. Young's moduli of  $Al_2TiO_5$ -mullite composites after thermal shock cycling.

strengths and Young's modulus were best described by Duckworth's exponential approach,<sup>16)</sup> where the open porosity had more effect on the modulus of elasticity than the closed porosity (comparable to ATM1 and ATM2 or ATM3). The ATM2-, ATM3-, and ATM5-composites show homogeneous microstructures with a defined microcrack system (see Fig. 1). This is grounds of the lower Young's modulus and with them lower flexural strength, but provided simultaneously excellent thermal shock resistance.

The lowest thermal expansion coefficient of studied materials was found at an  $Al_2TiO_5$ -content of 90 vol% (ATM1) and lies between  $0.5-2.0 \times 10^{-6} K^{-1}$  in the temperature range of RT-1200°C. Mullite additions of 10 vol% (ATM1) improved the strength of reaction-sintered material to 72 MPa with a low thermal expansion coefficient of  $0.5 \times 10^{-6} K^{-1}$ . This was attributed to the formation of a grain boundary liquid phase during sintering which aided densification and thus reduced microcracking, thereby in-

creasing the strength.

#### IV. Conclusions

The thermal expansion properties of the investigated Aluminium Titanate-Mullite composites show the hysteresis due to the strong anisotropy of  $\text{Al}_2\text{TiO}_5$ . These phenomena are explained by the opening and closing of microcracks. With decreasing the average grain size of 15  $\mu\text{m}$ , the hysteresis area was decreased. The difference in microcracking temperatures, e.g. 550, 700, and 800°C were caused by the difference in grain size. Young's modulus and flexural strength were maximum at a mullite content of 10 vol% but thermal shock resistance was minimum. The result can be attributed to a fewer grain boundary microcracks acting as a stress absorber.

#### References

1. W. R. Buessem, N. R. Thielke and R. V. Sarakauskas, "Thermal Expansion Hysteresis of Aluminium Titanate," *Ceram. Age*, **60**[5], 38-40 (1952)
2. J. A. Kuszyk and R. C. Bradt, "Influence of Grain Size on Effects of Thermal Expansion Anisotropy in  $\text{MgTi}_2\text{O}_6$ ," *J. of Am. Ceram. Soc.*, **56**[8], 420-423 (1973).
3. B. Morosin and R. W. Lynch, "Structure Studies on  $\text{Al}_2\text{TiO}_5$  at room Temperature and at 600°C," *Acta Cryst.*, **B28**, 1040 (1972).
4. G. Bayer, "Thermal Expansion Characteristics and Stability of Pseudobrookite-type Compounds  $\text{M}_3\text{O}_6$ ," *J. Fess. Common. Met.*, **24**, **2**, 129 (1971).
5. H. A. H. Thomas and R. Sterens, "Aluminium Titanate - A Literature Review, Part 1: Microcracking Phenomena," *Br. Ceram. Trans. J.*, **88**, 144 (1989).
6. Y. Ohya and Z. Nakagawa, "Grain Boundary Microcracking due to Thermal Expansion Anisotropy in Aluminium Titanate Ceramics," *J. Am. Ceram. Soc.*, **70**[8], C184 (1987).
7. I. J. Kim, "Anwendung des Sol-Gel-Verfahrens auf die Herstellung Keramischer Werkstoffe aus Aluminium Titanat - Mullit," Dissertation, Institut für Gesteinskundekunde, Techn. University Aachen, Germany (1991).
8. Ch. Hahn and D. Selb, "Verbesserung von Aluminiumtitanat - Keramik," *Sprechsaal*, **188**[12], 1157 (1985)
9. E. Gugel, "Keramische Konstruktionswerkstoffe fuer den Motorenbau," *Keramische Zeitschrift*, **36**, **9**, 477-479 (1984).
10. K. Uppenbrock, "Keramik in Motoren und Gasturbinen," *Sprechsaal*, **121**, **2**, 135-139 (1988).
11. W. Staudt, "Einfluss unterschiedlicher Dotierungen auf Eigenschaften und Gefuege von Geschmolzenem Aluminiumtitanat," Dissertation, RWTH Aachen (1988).
12. J. K. Kuszyk and R. G. Bradt, "Influence of Grain Size on Effects of Thermal Expansion Anisotropy in  $\text{MgTi}_2\text{O}_6$ ," *J. Am. Ceram. Soc.*, **56**[8], 420 (1973)
13. DIN 51068, Teil 1: Bestimmung des widerstandes gegen schroffen Temperaturwechsel - Wasserscheckverfahren für feuerfeste Steine, (1980).
14. B. Freudenberg, H. A. Linder, E. Gugel and P. Thometzek, "Thermomechanical Properties of Aluminium Titanate Ceramic between 20 and 1000°C," *ECRS*, **2**, **2**, 64-2, 71 (1989).
15. A. O. P. Hesse, "Temperturwechselbest Ndiges Feinporeses MgO - teil-stabilisiertes  $\text{ZrO}_2$ ," Dissertation TU clausthal (1988).
16. D. P. H. Hasselmann, "Unified Theory of Thermal Shock Fracture Initiation and Crack Propagation in Brittle Ceramics," *J. Am. Ceram. Soc.*, **36**, 68 (1953).